

STUDY OF THE INTERACTION OF NARINGENIN, APIGENIN, AND MENADIONE WITH MEMBRANES USING FLUORESCENT PROBES AND QUANTUM CHEMISTRY

A. G. Veiko,* E. A. Lapshina, H. G. Yuxhnevich, and I. B. Zavodnik

UDC 577.352.2+577.332+577.29

Quantum-chemical modeling of the optimal geometries of naringenin, apigenin, and menadione was performed. Their electronic properties and interactions with artificial liposomal membranes were evaluated using fluorescence probe spectroscopy. The studied flavonoids and quinone interacted strongly with 1,2-dimyristoyl-sn-glycero-3-phosphatidylcholine liposomal membranes according to the fluorescence analysis. The fluorescent probes TMA-DPH and DPH incorporated in the lipid bilayer were used to show that apigenin and naringenin (5–50 μM) and menadione (50 μM) decreased the microfluidity of the liposomal membrane bilayer at different depths with apigenin (but not menadione and naringenin) effectively quenching the fluorescence of TMA-DPH and DPH. Interaction of the studied compounds with the membranes depended on the polarity, volume, geometry, and water solubility of the molecules. The probe Laurdan was used to show that naringenin and apigenin dose-dependently converted the bilayer into a more ordered state while apigenin decreased the ordering of the lipid packing and increased the hydration near the polar head groups due to incorporation of the effectors into the liposomes. The torsion angle between the rings of the planar menadione and apigenin molecules was 180° while that of naringenin was 86.4° . Cranberry flavonoid glycosides (25–50 $\mu\text{g/mL}$) slightly increased the microfluidity of the liposomal membrane near the polar head groups of the phospholipids.

Keywords: flavonoids, naringenin, apigenin, menadione, liposome, fluorescence spectroscopy, quantum-chemical modeling, Stern–Volmer constant, fluorescent probe.

Introduction. Flavonoids are secondary metabolites of higher plants, are not synthesized in animal tissues, are characterized by an enormous variety of chemical structures, and demonstrate many beneficial biochemical and pharmacological effects in both *in vivo* and *in vitro* experiments [1]. Flavonoids as a class of plant polyphenols are characterized by the general diphenylpropane structure C6–C3–C6. Natural phenolic compounds vary structurally from simple phenols to complicated polymers and are not only simple antioxidants but also modulators of highly specific intracellular reactions and signaling pathways [2]. Model and epidemiological investigations showed that flavonoids, their metabolites, and synthetic derivatives possess several important pharmacological properties that prevent the development of neurological, cardiovascular, and oncological diseases [1, 3, 4]. Previously, the beneficial protective effects of flavonoids for diabetes [5] and toxic liver damage [6] and antibacterial activity [7] were studied by us. The molecular and cellular mechanisms of the biochemical and pharmacological effects of flavonoids are being actively investigated. The antimutagenic and anti-inflammatory potential of polyphenols and their antioxidant activity and ability to detoxify free radicals are well known. Flavonoids efficiently regulate the redox balance of cells, many cellular signaling pathways, and expression of certain genes. However, detailed information on the metabolism of flavonoids and quinones, the mechanisms of chemical transformations *in vitro* and *in vivo*, the formed intermediates, and the interactions with cellular structures and signaling cascades is missing. This limits their pharmacological use. The biochemical effects of flavonoids are mainly determined by their direct interactions with proteins and membranes. The present work evaluated the interaction parameters of selected flavonoids, i.e., the flavone apigenin and flavanone naringenin, which are broadly represented in the human diet, and the quinone menadione with artificial liposomal

*To whom correspondence should be addressed.

bilayer membranes produced from 1,2-dimyristoyl-*sn*-glycero-3-phosphatidylcholine (DMPC) using fluorescent probes incorporated into the liposomal membranes. The flavonoids naringenin and apigenin are secondary plant metabolites and exhibit various biological activities. The interaction with the membranes of a quinone, i.e., the lipophilic aromatic ketone menadione (vitamin K₃), was examined in addition to the polyphenols (flavonoids). The cytotoxicity of flavonoids, which is mostly determined by their prooxidant activity, is known to be related to the formation of free radicals and oxidation products, i.e., quinones. The cytotoxicity increases in concert with a reduction of the redox potential of the semiquinone/hydroquinone pair (the phenoxyl-radical/phenol pair) and an increase of the flavonoid lipophilicity [8].

Menadione (2-methyl-1,4-naphthoquinone) is a polycyclic aromatic ketone (vitamin K) that is reduced to the corresponding phenol in a redox cycle. Menadione is a promising chemotherapeutic agent and is readily incorporated into membrane systems, changing the organization of membrane structures. The high reactivity of menadione is responsible for its high toxicity [9]. Menadione was shown to interact directly with the membrane pump NorA protein. Incorporation of menadione into bacterial cell membranes changed the organization of the membranes and the morphology of the bacterial cell [10].

The aim of the present work was to determine the electronic properties and mechanisms of interaction of the polyphenols (apigenin and naringenin) and the quinone (menadione) with membrane structures using fluorescence spectroscopy.

Experimental. Tris(hydroxymethyl)aminomethane (Tris-HCl); 6-lauroyl-*N,N*-dimethyl-2-naphthylamine (Laurdan; Sigma-Aldrich-Merck, USA-Germany); 1,6-diphenyl-1,3,5-hexatriene (DPH); *N,N,N*-trimethyl-4-(6-phenyl-1,3,5-hexatrien-1-yl)phenylammonium *p*-toluenesulfonate (TMA-DPH, Molecular Probes, USA); apigenin (4',5,7-trihydroxyflavone); naringenin (Toronto Research Chemicals, Canada); menadione (Chem-Impex Intl. Inc., USA); and 1,2-dimyristoyl-*sn*-glycero-3-phosphatidylcholine (DMPC, Avanti Polar Lipids, USA) were used in the work. NaCl, NaH₂PO₄, Na₂HPO₄, and organic solvents were analytical grade (Lenreaktiv, Reakhim, Russia) and were used without further purification. The flavonoid complex was isolated from cranberry fruit as before [11]. The total content of polyphenols was 480 mg per 100 g of lyophilized extract. Freshly prepared solutions of the flavonoid complex in phosphate buffered saline (PBS, 145 mM NaCl, 1.9 mM NaH₂PO₄, 8.1 mM Na₂HPO₄, pH 7.4) at a concentration of 300 µg/mL and freshly prepared solutions of flavonoids (5 mM) and menadione in EtOH were used.

Liposomes (bilayer closed vesicles) of DMPC (14:0) were prepared by extrusion using a mini extruder (Avanti Polar Lipids, USA) as before [12]. A CHCl₃/lipid mixture was evaporated under N₂. The resulting thin lipid film was dissolved in PBS (pH 7.4) by heating to 45°C. The lipid suspension was filtered and passed 15 times through an extruder polycarbonate membrane (100-nm pore diameter) to produce a homogeneous liposome suspension. The final liposome concentration was 100 µg/mL.

The structure of the artificial liposome membranes was analyzed using fluorescence anisotropy of the probes 1,6-diphenyl-1,3,5-hexatriene (DPH) and *N,N,N*-trimethyl-4-(6-phenyl-1,3,5-hexatrien-1-yl)phenylammonium *p*-toluenesulfonate (TMA-DPH). DPH was dissolved in THF; TMA-DPH, in MeOH. The initial concentration of the probe was 1 mM. Liposomes (100 µg/mL) were incubated with DPH or TMA-DPH at a final concentration of 1 µM for 20 min at 25°C in PBS at pH 7.4. Fluorescence anisotropy was recorded with and without the flavonoids (Perkin-Elmer LS 55B fluorescence spectrometer, Great Britain). Changes of membrane microfluidity after adding the polyphenols and menadione were determined from the fluorescence anisotropy (r) calculated by the program for controlling the fluorescence spectrometer parameters:

$$r = \frac{I_{VV} - GI_{VH}}{I_{VV} + 2GI_{VH}},$$

where I_{VV} and I_{VH} are the vertical and horizontal fluorescence intensities for vertical polarization of the exciting light flux; G , correction factor for monochromator polarization effects; $G = I_{HV}/I_{HH}$, where I_{HV} and I_{HH} are the vertical and horizontal fluorescence intensity for horizontal polarization of the exciting light flux. The results were given as the ratio r_s/r_0 , where r_s and r_0 are the fluorescence anisotropy of the probes with and without polyphenols. The excitation and emission wavelengths were 348 and 426 nm for DPH; 340 and 430 nm for TMA-DPH.

The structure and hydration of the liposomal membranes were analyzed using Laurdan fluorescent probe. Laurdan was dissolved in DMSO (1 mM) and incubated in a suspension of the liposomal membranes (100 µg/mL) in PBS at pH 7.4 for 15 min at 37°C to allow the probe to incorporate into the membrane. The final probe concentration was 0.3 µM. Laurdan fluorescence was recorded using a Perkin-Elmer LS 55B fluorescence spectrometer (Great Britain). Generalized

polarization (GP) of Laurdan was calculated using the formula $GP = (I_{460} - I_{490}) / (I_{440} + I_{490})$, where I_{440} and I_{490} are probe fluorescence intensities upon excitation at 350 nm recorded at 440 and 490 nm. Laurdan fluorescence was sensitive to the local polarity and reflected a change in the condition and hydration of the membrane because of coupling of the probe dipole moment and its fluorescence spectrum. The degree of hydration was estimated from the fluorescence GP [13].

Calculations. Quantum-chemical parameters and molecular geometry were calculated using HyperChem 8.0 computational software (Hypercube Inc., USA) based on the AM1 (The Austin Model 1) semi-empirical method and an *ab initio* method with basis set 6-31G and the Polak-Ribiere algorithm, which computed the optimal molecular conformation with the minimal energy-distribution gradient in a vacuum. Experimental results as averages \pm standard deviations were checked for normal distributions using the Shapiro-Wilk criterion. Differences between parameters measured in groups with normal distributions were analyzed using the Student criterion. If the data distribution deviated from normal, then the statistical significance of differences between parameters measured in groups were analyzed using the Mann-Whitney nonparametric criterion. Data were statistically processed using GraphPad and StatSoft Statistica programs. The significance parameter was set at the level $p < 0.05$.

Results and Discussion. The quantum-chemical parameters of naringenin, apigenin, and menadione were computed because the electronic and molecular parameters of flavonoids and quinones are highly significant for biochemical and pharmacological activity (Table 1). Figure 1 shows the optimized geometries of the molecules. Rings *AC* and *B* in apigenin (but not naringenin) were situated in the same plane. The torsion angle $C3-C2-C1'-C2'$ was 180° . The apigenin molecule was planar probably because of the $C2=C3$ double bond in the *C*-ring. The menadione molecule also was planar. According to AM1 calculations, the dipole moment of the studied molecules increased in the order menadione < naringenin < apigenin (Table 1), which reflected the efficiency of electrostatic interactions of the molecules with the surroundings. The apigenin molecule had the lowest LUMO energy (lower unoccupied molecular orbital, i.e., free orbital with the lowest energy). Therefore, it acted as an effective electron acceptor during attack by nucleophiles.

The binding parameters of selected agents with the liposomes were estimated to reveal the physicochemical nature of the interactions of flavonoids and quinones with phospholipid membranes. For this, the fluorescence intensities and anisotropies of the lipophilic fluorescent probes DPH and TMA-DPH and Laurdan GP probe were used. It seemed interesting to determine the relationship of the structures of the studied compounds and their effects on the condition of the investigated membranes. Changes in the microfluidity of the lipid bilayer membranes in the presence of the flavonoids and menadione were determined using DPH and TMA-DPH with different localizations in the membrane bilayer. The TMA-DPH probe was localized at the water/membrane interface near the phospholipid polar heads. The DPH probe distributed in the hydrophobic part of the liposomal membranes occupied by the phospholipid hydrocarbon chains. Fluorescence anisotropy of these probes reflected changes in the mobility of the probes and was proportional to the rigidity of the bilayer and its ordering.

The experimental results were given as functions of the ratio (r_s/r_0) of the fluorescence anisotropies of the DPH and TMA-DPH probes incorporated into the lipid bilayer (Fig. 2) on the polyphenol concentration. Measurements of the fluorescence anisotropy of the DPH and TMA-DPH probes showed that the lipophilic flavonoid apigenin interacted directly with DMPC liposomal membranes, significantly increasing r_s/r_0 dose-dependently for both probes (5–50 μM) and decreasing the fluidity of the lipid bilayer (increasing the ordering and rigidity) at both the water/membrane interface and near the lipid hydrocarbon chains. The effect of apigenin was more pronounced for TMA-DPH fluorescence than for that of DPH. This indicated that the flavonoid was localized primarily in the membrane surface region. The increase of membrane rigidity in the presence of flavonoids was reported to prevent diffusion of free radicals and to inhibit lipid peroxidation [14]. Naringenin also increased the membrane rigidity at the water-lipid-bilayer interface although to a lesser extent. The effect of naringenin on the internal hydrophobic membrane region was even less evident. Water-insoluble menadione also changed the lipid bilayer organization and increased the rigidity at the water-bilayer interface, decreasing the rigidity of the internal membrane region at low (5–10 μM) and increasing the rigidity at high concentrations (50 μM). It could be assumed by comparing the molecular parameters of apigenin, naringenin, and menadione and their effects on the membrane structure and dynamics that the interaction with the lipid bilayer was determined by the molecular geometry, volume, polarity, and dipole moment.

The effects of the flavonoids and menadione on the fluorescence parameters of DPH and TMA-DPH were compared with the effects on the fluorescence parameters of Laurdan incorporated into the liposomal membranes. The fluorophore Laurdan was localized in the membrane at the level of the phospholipid glycerin moiety. Changes of Laurdan GP are known to be related to changes of the dipole moment and reflect the degree of hydration of lipids at the water-lipid interface of

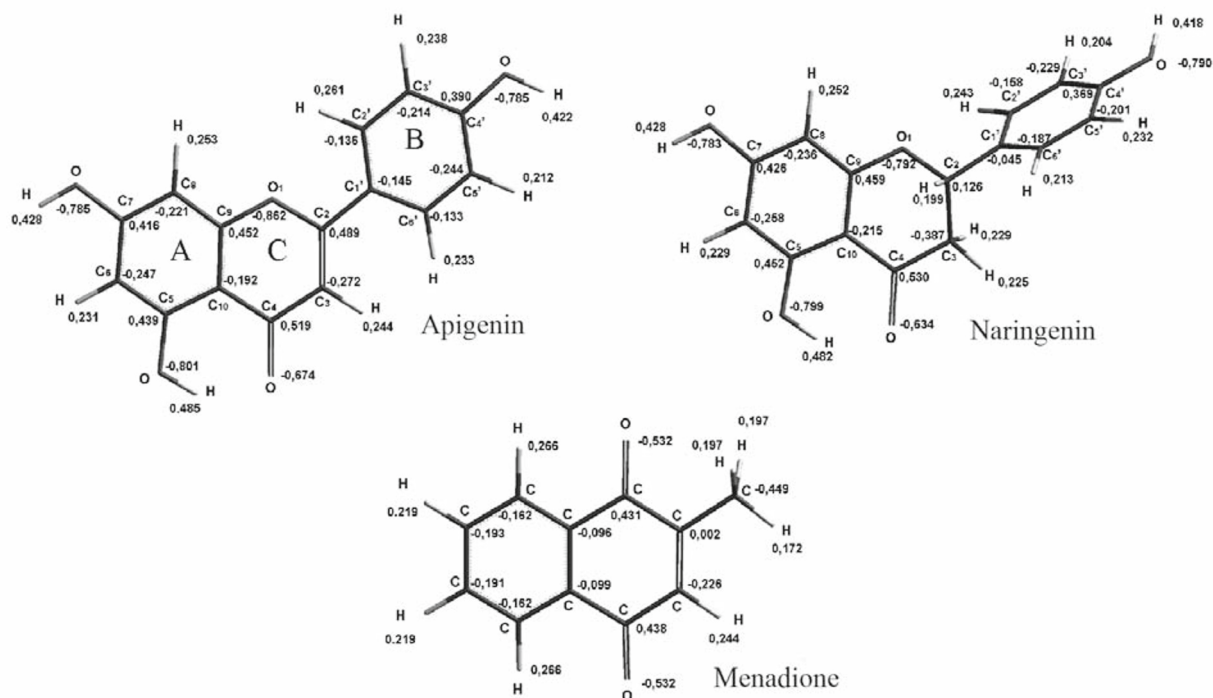


Fig. 1. Optimized molecular structure and atomic charge excesses in apigenin, naringenin, and menadione molecules calculated by a nonempirical *ab initio* method using basis set 6-31G and unrestricted Hartree–Fock method in self-consistent field approximation and Polak–Ribiere algorithm.

TABLE 1. Quantum-Chemical Parameters and Torsion Angles of Naringenin, Apigenin, and Menadione Molecules

Parameter	Naringenin	Apigenin	Menadione
AM1 UHF			
Number of electrons	102	100	64
Total energy, kcal/mol	-85,033.734	-84,380.214	-49,768.600
Bond energy, kcal/mol	-3640.1191	-3512.2053	-2439.4955
Heat of formation, kcal/mol	-153.750	-130.040	-23.772
Dipole moment, D	1.602	2.123	1.093
QSAR properties			
Volume, Å ³	736.63	719.5	525.1
Hydration energy, kcal/mol	-22.97	-23.63	-1.28
<i>ab initio</i> UHF (6-31G)			
E (HOMO), eV	-8.8522	-8.6236	-9.7791
E (LUMO), eV	2.0381	1.4850	2.6751
$\Delta E = E(\text{HOMO}) - E(\text{LUMO})$, eV	-10.8903	-10.1086	-12.4542
Torsion angles, deg	86.4	180	180

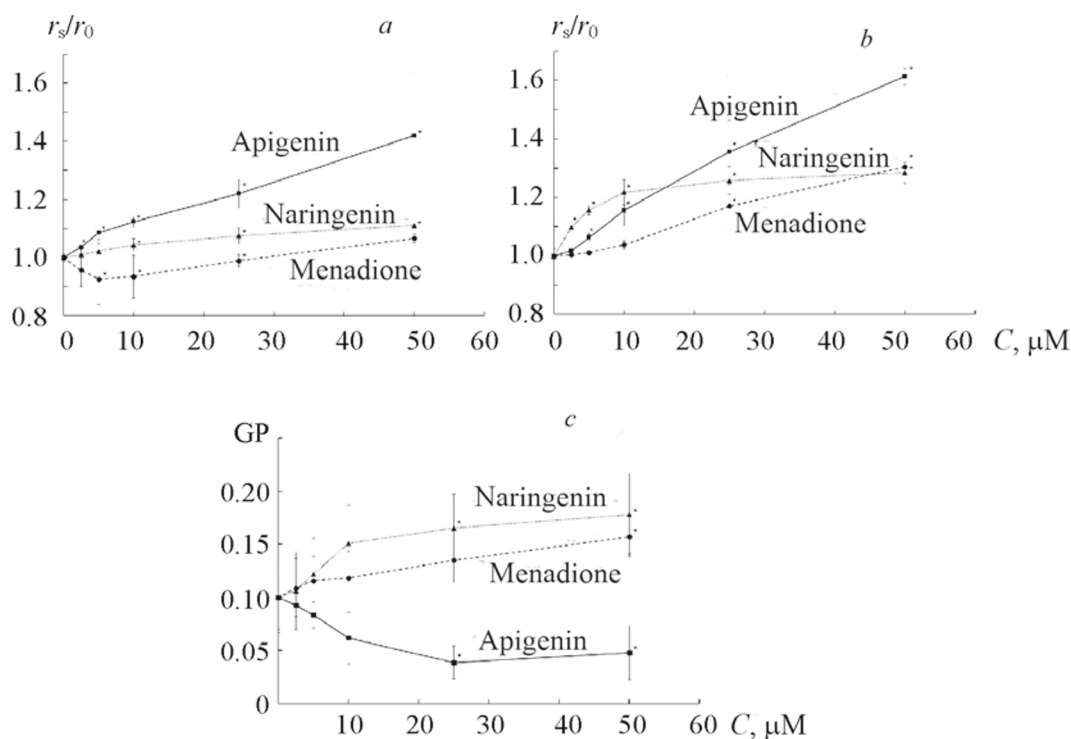


Fig. 2. Dependences of fluorescence anisotropy of DPH probes situated in the membrane hydrophobic part (a), TMA-*DPH* localized at the water-bilayer interface (b), and GP of Laurdan probe incorporated into liposomal membranes (c) on concentration of menadione, naringenin, and apigenin; liposomes (100 μg/mL) were incubated with DPH and TMA-*DPH* (1 μM) for 20 min at 25°C and with Laurdan (0.3 μM) for 5 min at 37°C in PBS, pH 7.4; $\lambda_{\text{ex}} = 348$ nm, $\lambda_{\text{em}} = 426$ nm for DPH (a) and TMA-*DPH* (b); fluorescence intensity for Laurdan (c) was recorded at 440 and 490 nm after fluorescence excitation at $\lambda = 350$ nm; $p < 0.05$ vs. liposomal membranes without flavonoids and menadione.

TABLE 2. Stern-Volmer Constants K_{SV} for Quenching of TMA-*DPH* and DPH Probe Fluorescence by Naringenin, Apigenin, and Menadione Incorporated into Liposomal Membranes and Solubility of Naringenin, Apigenin, and Menadione

$K_{\text{SV}}, \text{M}^{-1}$	Naringenin	Apigenin	Menadione
DPH probe	$(0.13 \pm 0.01) \cdot 10^5$	$(1.62 \pm 0.05) \cdot 10^5$	$(0.04 \pm 0.01) \cdot 10^5$
TMA- <i>DPH</i> probe	$(0.28 \pm 0.03) \cdot 10^5$	$(2.12 \pm 0.06) \cdot 10^5$	$(0.13 \pm 0.02) \cdot 10^5$
Water solubility, mg/L	4.38 [16]	2.16 [17]	insoluble [18]

liposomal membranes [13]. Figure 2c shows that the flavonoids and menadione had different effects. Naringenin, like menadione, increased the Laurdan GP, indicative of dehydration of the lipid bilayer. Apigenin significantly decreased it, probably because of an increase in the degree of hydration of the membrane lipid bilayer and a transition of the membrane from a solid ordered phase into a liquid disordered phase in the presence of this flavonoid [15].

Incorporation of the effector molecules (flavonoids apigenin and naringenin and quinone menadione) into the membranes was also evaluated from the quenching efficiency by them of the fluorescence of DPH and TMA-*DPH* probes incorporated into the liposomes. Figure 3 shows dependences of quenching by apigenin, naringenin, and menadione of the fluorescence of DPH and TMA-*DPH* probes incorporated into the liposomal membranes in Stern-Volmer coordinates.

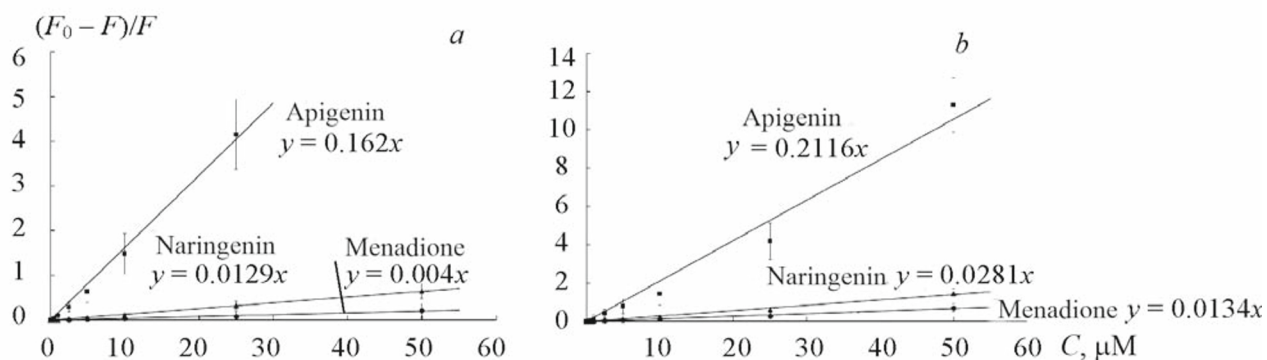


Fig. 3. Dependences of fluorescence quenching of DPH (a) and TMA–DPH probes (b) incorporated into liposomal membranes plotted in Stern–Volmer coordinates, where F_0 and F are fluorescence intensities of the probe, on effectors; liposomes (100 $\mu\text{g}/\text{mL}$) were incubated with DPH and TMA–DPH (1 μM) for 20 min at 25°C, PBS, pH 7.4; effectors were incubated with liposomes for 5 min at 25°C after incorporation of the probes; $\lambda_{\text{ex}} = 348 \text{ nm}$, $\lambda_{\text{em}} = 426 \text{ nm}$; $p < 0.05$ vs. liposomal membranes without effectors.

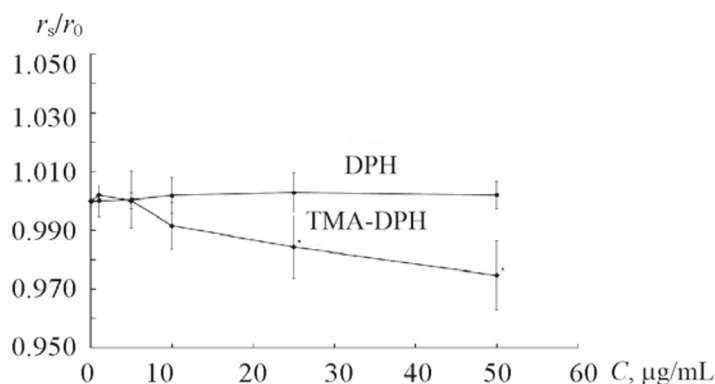


Fig. 4. Dependences of fluorescence anisotropy of DPH and TMA–PDH probes incorporated into liposomal membranes on cranberry fruit flavonoid content; liposomes (100 $\mu\text{g}/\text{mL}$) were incubated with DPH and TMA–DPH (1 μM) for 20 min at 25°C, PBS, pH 7.4; flavonoids were incubated with liposomes for 5 min at 25°C after incorporation of the probes; $\lambda_{\text{ex}} = 348 \text{ nm}$, $\lambda_{\text{em}} = 426 \text{ nm}$; $p < 0.05$ vs. liposomal membranes without flavonoids.

The Stern–Volmer constants K_{SV} were significantly greater for fluorescence quenching by apigenin than by naringenin and menadione (Table 2). The flavonoid apigenin with the largest dipole moment and a planar structure, penetrated most effectively into the lipid bilayer. Also, the quenching efficiency of the probe incorporated into the membranes at the water–lipid-bilayer interface (TMA–DPH) was greater than that of the probe localized in the internal membrane regions (DPH) for all studied quencher molecules.

The parameters for the interaction of the flavonoid complex isolated from cranberry fruit with the liposomal membranes were evaluated. The flavonoids primarily as glycosides at concentrations of 25–50 $\mu\text{g}/\text{mL}$ insignificantly decreased r_s/r_0 for TMA–DPH probe localized at the water–bilayer interface and did not affect this parameter for DPH probe situated in the hydrophobic part of the membrane (Fig. 4). The affinity of flavonoids for membranes and their membrane permeability are known to be determined by the degree of hydroxylation, the molecular configuration, and the length of the side chain [19]. One mechanism for the beneficial therapeutic effects of plant polyphenols may be their modulating effect on the condition and dynamics of membrane lipid bilayers. Incorporation and distribution of the polyphenols and the quinone

into membranes in our experiment changed the biophysical characteristics of the membrane. This was manifested in the pronounced changes of the fluorescence characteristics of the probes incorporated into the membranes. Previously, interaction of the flavonoid quercetin with a lipid bilayer was shown to have a dual mechanism of action [20]. The polyphenol was distributed in membrane liquid domains that were more vulnerable to oxidative attack and simultaneously induced strong perturbations of domains enriched in cholesterol/sphingolipid where signaling platforms were assembled. Measurements of the fluorescence anisotropy of TMA–DPH and DPH probes showed that the lipophilic flavonoid apigenin and to a lesser extent naringenin and menadione interacted directly with liposomal membranes and dose-dependently decreased the microfluidity (increased the rigidity) at various depths of the membrane lipid bilayer. The flavonoids had a significantly greater effect on the rigidity of the membrane hydrophobic region than on the water–membrane interface. Previously, it was proposed that polyphenols interact mainly with the glycerin moiety and the acyl-chain region of membranes [21]. It was demonstrated that incorporation of flavonoids into membranes can imitate the action of cholesterol in membranes and promote the formation of membrane microdomains [22]. The cranberry fruit flavonoid complex in our experiment, which was primarily glycosylated species, insignificantly increased the mobility of the phospholipids in the surface layer and did not affect the organization of membrane internal regions, in contrast to the aglycons naringenin and apigenin.

Conclusions. Changes in the fluorescence parameters of the probes TMA–DPH, DPH, and Laurdan incorporated into membrane lipid bilayers enabled an evaluation of the effects of polyphenols (apigenin and naringenin) and quinones (menadione) on the structure and physicochemical characteristics of membranes. Quantum chemistry was used to estimate the geometry and electronic properties of apigenin, naringenin, and menadione. The probes DPH, TMA–DPH, and Laurdan had different localizations in the membrane bilayer. Fluorescence anisotropy of DPH and TMA–DPH reflected changes of probe mobility and was proportional to the lipid bilayer rigidity and its ordering. Laurdan GP reflected the degree of hydration of lipids at the water–lipid interface of the liposomal membranes. Incorporation of flavonoids and quinones into the bilayer of unilamellar liposomes changed the packing ordering of phospholipids, the degree of mobility of phospholipids, and the water content in the bilayer. The lipophilic flavonoid apigenin dose-dependently (5–50 μM) increased the ordering and rigidity of the lipid bilayer both at the water–membrane interface and in the lipid hydrocarbon-chain region. Naringenin to a much lesser extent increased the membrane rigidity at the water–lipid-bilayer interface. Water-insoluble menadione increased the rigidity at the water-bilayer interface, decreased the rigidity of the membrane internal region at low concentrations, and increased it at high concentrations. The quinone menadione had a weaker effect than the polyphenols. It could be assumed by comparing the molecular parameters of apigenin, naringenin, and menadione and their effects on the membrane structure and dynamics that the interaction with the lipid bilayer was determined by the molecular geometry, volume, polarity, and dipole moment. Thus, the high biological activities of the flavonoids and menadione were associated with modulation of the biophysical and biochemical parameters of biological membranes.

REFERENCES

1. A. N. Panche, A. D. Diwan, and S. R. Chandra, *J. Nutr. Sci.*, **5**, e47 (2016).
2. F. Shahidi and P. Ambigaipalan, *J. Funct. Foods*, **18**, 820–897 (2015).
3. D. M. Kopustinskiene, V. Jakstas, A. Savickas, and J. Bernatoniene, *Nutrients*, **12**, No. 2, 457 (2020).
4. Y. Xie, W. Yang, F. Tang, X. Chen, and L. Ren, *Curr. Med. Chem.*, **22**, No. 1, 132–149 (2015).
5. V. Buko, I. Zavodnik, O. Kanuka, E. Belonovskaya, E. Naruta, O. Lukivskaya, S. Kirko, G. Budryn, D. Zyzelewicz, J. Oracz, and N. Sybirna, *Food Funct.*, **9**, No. 3, 1850–1863 (2018).
6. V. Buko, E. Belonovskaya, T. Kavalenia, T. Ilyich, S. Kirko, I. Kuzmitskaya, V. Moroz, E. Lapshina, A. Romanchuk, and I. Zavodnik, *Eur. Pharm. J.*, **69**, No. 2, 5–16 (2022).
7. A. G. Veiko, E. Olchowik-Grabarek, S. Sekowski, A. Roszkowska, E. A. Lapshina, I. Dobrzynska, M. Zamaraeva, and I. B. Zavodnik, *Molecules*, **28**, No. 3, 1252 (2023).
8. A. Marozienne, A. Nemeikaite-Ceniene, R. Vidziunaite, and N. Cenas, *Acta Biochim. Pol.*, **59**, No. 2, 299–305 (2012).
9. J. P. Monteiro, A. F. Martins, C. Nunes, C. M. Morais, M. Lucio, S. Reis, T. J. T. Pinheiro, C. F. G. C. Gerales, P. J. Oliveira, and A. S. Jurado, *Biochim. Biophys. Acta, Biomembr.*, **1828**, No. 8, 1899–1908 (2013).
10. S. R. Tintino, V. C. A. de Souza, J. M. A. da Silva, C. D. de M. Oliveira-Tintino, P. S. Pereira, T. C. Leal-Balbino, A. Pereira-Neves, J. P. Siqueira-Junior, J. G. M. da Costa, F. F. G. Rodrigues, I. R. A. Menezes, G. C. A. da Hora, M. C. P. Lima, H. D. M. Coutinho, and V. Q. Balbino, *Membranes*, **10**, No. 6, 130 (2020).

11. E. A. Lapshina, M. Zamaraeva, V. T. Cheshchevik, E. Olchowik-Grabarek, S. Sekowski, I. Zukowska, N. G. Golovach, V. N. Burd, and I. B. Zavodnik, *Cell Biochem. Funct.*, **33**, No. 4, 202–210 (2015).
12. A. G. Veiko, S. Sekowski, E. A. Lapshina, A. Z. Wilczewska, K. H. Markiewicz, M. Zamaraeva, H. Zhao, and I. B. Zavodnik, *Biochim. Biophys. Acta, Biomembr.*, **1862**, No. 11, 183442 (2020).
13. S. A. Sanchez, M. A. Tricerri, and E. Gratton, *Proc. Natl. Acad. Sci. USA*, **109**, No. 19, 7314–7319 (2012).
14. A. Arora, T. M. Byrem, M. G. Nair, and G. M. Strasburg, *Arch. Biochem. Biophys.*, **373**, No. 1, 102–109 (2000).
15. S. V. Verstraeten, G. K. Jagers, C. G. Fraga, and P. I. Oteiza, *Biochim. Biophys. Acta, Biomembr.*, **1828**, No. 11, 2646–2653 (2013).
16. J. Wen, B. Liu, E. Yuan, Y. Ma, and Y. Zhu, *Molecules*, **15**, No. 6, 4401–4407 (2010).
17. W. Alam, C. Rocca, H. Khan, Y. Hussain, M. Aschner, A. De Bartolo, N. Amodio, T. Angelone, and W. S. Cheang, *Antioxidants*, **10**, No. 10, 1643 (2021).
18. https://www.acros.com/DesktopModules/Acros_Search_Results/Acros_Search_Results.aspx?search_type=CatalogSearch&SearchString=menadione (accessed Mar. 7, 2023).
19. P. Tammela, L. Laitinen, A. Galkin, T. Wennberg, R. Heczko, H. Vuorela, and J. P. Slotte, *Arch. Biochem. Biophys.*, **425**, No. 2, 193–199 (2004).
20. A. de Granada-Flor, C. Sousa, H. A. L. Filipe, M. S. C. S. Santos, and R. F. M. de Almeida, *Chem. Commun.*, **55**, No. 12, 1750–1753 (2019).
21. O. Wesolowska, J. Gasiorowska, J. Petrus, B. Czarnik-Matusiewicz, and K. Michalak, *Biochim. Biophys. Acta, Biomembr.*, **1838**, No. 1, 173–184 (2014).
22. Y. S. Tarahovsky, E. N. Muzafarov, and Y. A. Kim, *Mol. Cell Biochem.*, **314**, No. 1, 65–71 (2008).